Calcium- and BTB domain protein-modulated PINOID protein kinase directs polar auxin transport

Robert-Boisivon, H.S.

Chapter 3

Cell-type and tissue-specific regulation of PID signaling by small calcium-binding proteins

Hélène Robert, Yang Xiong[1], Remko Offringa

[1] Current address: College of Life Sciences, Peking University, Beijing 100871, China

Abstract

The plant hormone auxin regulates plant development and tropic growth responses through its unidirectional transport, creating auxin gradients and maxima that are instrumental for basic cellular processes such as elongation, differentiation and division. The direction of this intercellular auxin transport is determined by the asymmetric localization of PIN auxin transporters whose subcellular targeting is dependent on their phosphorylation by the protein serine/threonine kinase PINOID (PID). Here we investigated the role of two small calcium-binding proteins, PINOID BINDING PROTEIN1 (PBP1) and its close homolog, whose interaction with PID is enhanced by calcium. Genetic experiments with different loss- and gain-of-function lines indicate that PBP1 and PBP1H act redundantly to enhance PID activity during embryo development, and that they suppress root growth, possibly through their stimulatory effect on PID. *PBP1* overexpression partially inhibits the auxin-induced calcium-dependent sequestration of PID from the plasma membrane, indicating that apart from enhancing the activity of the PID kinase, PBP1 also stabilizes the association of PID with the plasma membrane, close to the PIN phosphorylation targets. Interestingly, *pbp1-1* loss-of-function partially rescues the inflorescence phenotypes of the *pid-14* mutant allele, which seemingly contradicts the role of PBP1 as positive regulator of PID activity. We conclude that PBP1 and PBP1H fine-tune PID signaling in response to changes in cytosolic calcium, in a cell-type and tissue-specific manner.

Introduction

Auxin plays important roles as informative molecule in many cellular processes and in plant development (reviewed in Tanaka et al., 2006). Intercellular polar auxin transport (PAT) generates auxin gradients and maxima, essential for tropic growth responses, embryogenesis, organ positioning and meristem maintenance (Sabatini et al., 1999, Friml et al., 2002, Friml et al., 2003, Reinhardt et al., 2003, Benková et al., 2003). Auxin transport is tightly regulated by the presence of the polar localized PIN efflux carriers (Tanaka et al., 2006). These transmembrane facilitator proteins are the rate limiting factors in auxin efflux (Petrášek et al., 2006) and determine the direction of PAT through their asymmetric subcellular localization (Wisniewska et al., 2006). The plant specific protein serine/threonine kinase PINOID (PID) regulates PAT by controlling PIN localization, and thereby determining the direction of PAT (Benjamins et al., 2001, Friml et al., 2004). Recent data indicate that PID is a plasma membrane-associated kinase that acts antagonistic to trimeric PP2A phosphatases, through direct phosphorylation of PINs (Lee and Cho, 2006, Michniewicz et al., 2007).

Calcium is a common second messenger in signaling pathways. Early studies on sunflowers stem sections showed that PAT was abolished by the presence of calcium chelators and restored by application of calcium solutions, which suggested an important role for calcium in the regulation of PAT (Dela Fuente and Leopold, 1973). The first molecular evidence for a link between calcium and PAT was provided by the identification of the calcium-binding proteins PINOID BINDING PROTEIN1 (PBP1) and TOUCH3 (TCH3) as interacting proteins of PID (Benjamins et al., 2003). The calcium-dependent binding of PBP1 and TCH3 to PID was found to respectively up-regulate and repress the PID kinase autophosphorylation activity in *in vitro* phosphorylation assays (Benjamins et al., 2003). Further analysis of the *in vivo* difference of the interaction between the calmodulin-related protein TCH3 and PID indicated that binding of TCH3 to the catalytic domain not only suppresses the activity of the kinase, but also sequesters the plasma membrane-associated kinase to the cytoplasm, away from the PIN phosphorylation targets (Chapter 2, this thesis). In contrast to TCH3, which has six calcium-binding pockets, or EF-hands, PBP1 has a single EF-hand. PBP1 is also known as KRP2 (for KIC-related protein2), as it is part of a small protein family that includes KIC (KCBP-interacting Calcium binding protein) and the close PBP1 homologue PBP1H/KRP1 (Reddy et al., 2004). KIC is involved in the regulation of trichome development by a calcium-dependent interaction with the kinesin-like calmodulin-binding protein KCBP (Reddy et al., 2004). KCBP is a microtubule (MT) motor protein that determines trichome morphology by regulating branching and polar growth (Reddy and Day, 2000). Calcium-dependent KIC-KCBP interaction inhibits binding of KCBP with the MT, thereby affecting trichome development (Reddy et al., 2004). Interestingly, this pathway also implicates KIPK, a KCBP-interacting protein kinase that belongs to the same AGCVIII kinase family as PID (Day et al., 2000, Lee and Cho, 2006, Galván-Ampudia and Offringa, 2007). Up to now, a direct interaction between KIC and KIPK, as shown for PBP1 and PID, has not been reported.

Here we present a more detailed functional and genetic analysis to further elucidate the regulatory role of PBP1 and its close homologue PBP1H in PID signaling. Experiments with combinations of loss- and gain-of-function mutant lines of *PBP1*, *PBP1H* and *PID* indicate that PBP1 and PBP1H act redundantly to enhance PID activity during embryo development, and that they partly suppress root growth, possibly through their stimulatory effect on PID. *PBP1* overexpression partially inhibits auxin-induced calcium-dependent sequestration of PID from the plasma membrane, suggesting that apart from enhancing the activity of the PID kinase, PBP1 also influences PID subcellular localization. These data confirm *in vitro* data, indicating a role for PBP1 and PBP1H as positive regulators of the PID kinase activity. Unexpectedly, however, *pbp1-1* loss-of-function was found to partially suppress *pid-14* inflorescence phenotypes, suggesting a repressing role for PBP1 on PID activity during inflorescence development. These seemingly contradictory

results imply that PBP1 and PBP1H have a cell-type and tissue-specific effect on the PID pathway.

Results

PBP1 *loss- and gain-of-function mutants are affected in root length*

Previously, PBP1/KRP2 was identified as an interactor of PINOID that enhances the *in vitro* autophosphorylation activity of this protein serine/threonine kinase (Benjamins et al., 2003). As a first approach to analyze the function of PBP1 as a regulator of the PID kinase activity *in planta*, we isolated the *pbp1-1* loss-of-function allele, and generated lines overexpressing the *PBP1* cDNA under control of the *35S* promoter.

The *pbp1-1* allele (line GT6553 in Landsberg *erecta* (L*er*) background) has a transposon inserted at 91bp after the ATG, before the region encoding the EF-hand domain (Figure 5A). RT-PCR analysis did not detect *PBP1* transcript in *pbp1-1* mutant seedlings, indicating that it is a complete loss-of-function allele (Figure 1A). Detailed phenotypic analysis revealed that the primary roots of *pbp1-1* were longer than wild type roots (120 % of the L*er* root length, Student's t-test, $p < 0.02$, Figure 1C). Apart from that, *pbp1-1* did not show any other phenotype, and since the expression of the closely homologous gene *PBP1H/KRP1* was not altered in *pbp1-1* (Figure 1A), this suggests that, except for a specific role for *PBP1* in root growth, *PBP1* and *PBP1H* act redundantly.

From the multiple overexpression lines that were generated, two single locus lines were selected for further studies: one with a strong (*35Spro:PBP1-29*) and one with a medium (*35Spro:PBP1-53*) *PBP1* overexpression level (Figure 1B). The only observed phenotype in these lines was a slight but significant reduction of the root length. The roots in the *35Spro:PBP1*-29 and *-53* were 86 % and 90 % of the wild type Col root length, respectively (Student's t-test, $p < 0.02$, Figure 1C). The root length reduction correlated with the level of overexpression of *PBP1* in these two lines. Seedlings of the two *PBP1* overexpressing lines still showed a significant reduction in root length when germinated on medium containing 0.1 µM of the auxin indole-3-acetic acid (IAA) or the auxin transport inhibitor naphthylphtalamic acid (NPA) (data not shown). Also other auxin-dependent responses such as root gravitropism or lateral root initiation were not affected (data not shown).

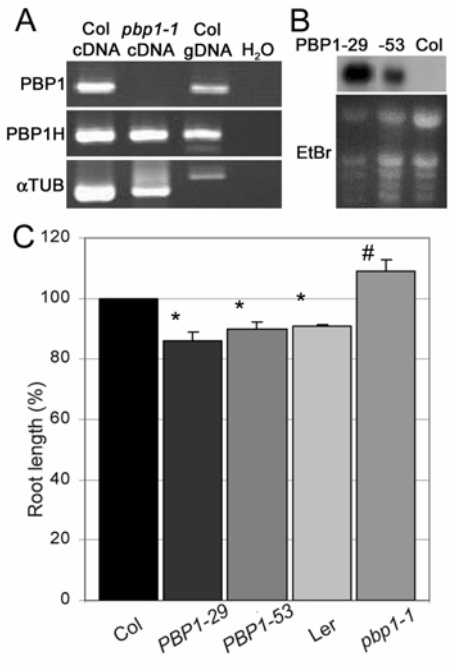

Figure 1. PBP1 represses root growth.
(A) RT-PCR on Col cDNA, *pbp1-1* cDNA and Col genomic DNA of one-week old seedlings indicates that *pbp1-1* is a null allele for *PBP1*, and that *PBP1H* expression is not affected.
(B) Northern blot analysis showing the level of *PBP1* overexpression in seedlings of the *PBP1* overexpression lines *35Spro:PBP1-29* and *-53*, as compared to Col wild type. The ethidium bromide stained RNA gel is shown as loading control.
(C) Percentage of root growth in eight day-old seedlings of *35Spro:PBP1-29* and *-53*, *pbp1-1* and L*er*, as compared to Col wild type. The mean of three experiments is shown, * significantly different from Col, # significantly different from L*er* (Student's t-test, $p < 0.02$).

PBP1 does not significantly influence the PID gain-of-function root collapse

To more specifically address the functionality of the PID-PBP1 interaction *in planta*, the *pbp1-1* allele and the two *PBP1* overexpression lines were crossed into the *35Spro:PID-21* overexpression line (Benjamins et al., 2001). The absence of auxin maxima in the root tip of *35Spro:PID-21*, due to a change of polarity of the PIN auxin efflux carriers localization, provokes differentiation of the main root meristem initials, thus leading to meristem collapse (Benjamins et al., 2001, Friml et al., 2004). This phenotype is not visible in all seedlings, but occurs gradually during seedling growth from three to six days after germination (dag). The percentage of seedlings showing the phenotype at a certain number of dag is a good measure for the PID activity- or overexpression levels. In line *35Spro:PID-21*, root collapse is observed in 6 % of the seedlings at three dag and in 96 % of the seedlings at five dag (Figure 2A) (Benjamins et al., 2001). In view of the positive effect of PBP1 on PID kinase activity *in vitro*, we expected *pbp1* loss-of-function to reduce and *PBP1* overexpression to enhance the root collapse phenotype.

The percentage of the root collapse in *35Spro:PID-21 pbp1-1* seedlings did not significantly differ from that in *35Spro:PID-21* seedlings (Figure 2A). For *PBP1* overexpression lines, a significant decrease of the *35Spro:PID*-induced root collapse was observed only at four dag (57 % and 45 % for *35Spro:PID-21 35Spro:PBP1-29* and *35Spro:PID-21 35Spro:PBP1-53*, respectively versus 82 % for *35Spro:PID-21*, Student's t-test, $p < 0.04$) (Figure 2A), but not at other time points. Since an increase rather than a

decrease of the root collapse penetrance was expected in the crossed lines due to the putative positive regulatory activity of PBP1, the level of expression of *PID* and *PBP1* was checked by Northern blot analysis. The *PID* overexpression levels were reduced to 48 % in *35Spro:PID-21 pbp1-1*, and this line did not show a significant change in root meristem collapse. We therefore are confident that the observed decrease in penetrance of the root collapse phenotype in the *35Spro:PID-21 35Spro:PBP1* seedlings is not due to a significant

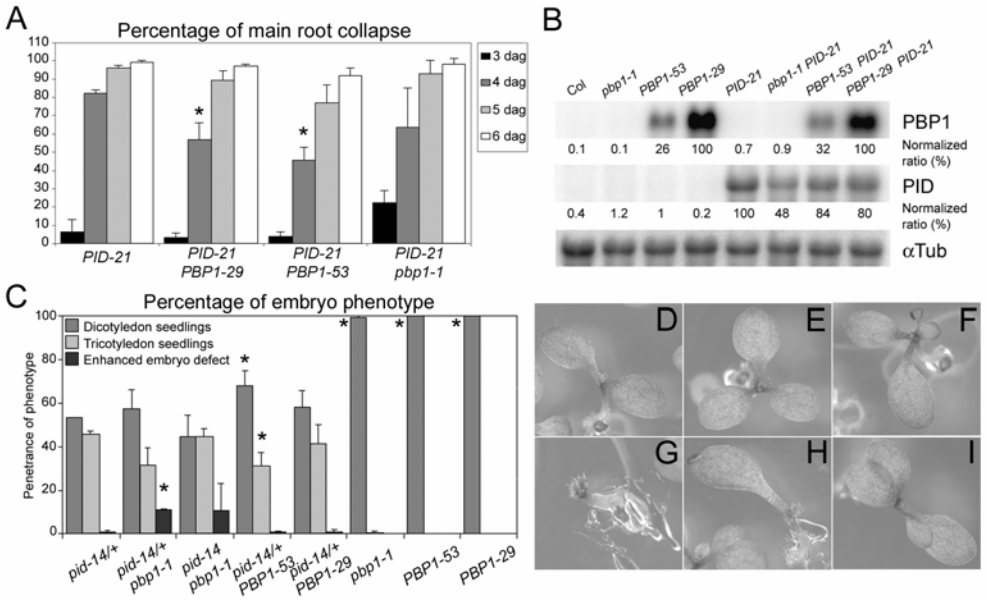

Figure 2. *pbp1-1* loss-of-function enhances *pid-14* embryo phenotypes.

(A) Graph showing the percentage of main root meristem collapse at 3, 4, 5 and 6 days after germination (dag) in *35Spro:PID-21* (n = 78, 117, 110), *35Spro:PID-21 35S: PBP1-29* (n = 201, 202, 235), *35Spro:PID-21 35Spro:PBP1-53* (n = 190, 244, 239) and *35Spro:PID-21 pbp1-1* (n = 58, 104, 102). Stars (*) indicated that the values are significantly different compared to *35Spro:PID-21* (Student's t-test, $p < 0.04$).

(B) Expression analysis of *PID* and *PBP1* by Northern blots showing that *PBP1* overexpression is strongest in line *35Spro:PBP1-29*, and that there are slight variations in the *PID* overexpression levels between the overexpression lines analyzed in (A).

(C) The percentage of cotyledon phenotypes in progeny of *pid-14/+* (n = 1469), *pid-14/+ pbp1-1* (n = 1040), *pid-14 pbp1-1* (n = 291), *pid-14/+ 35Spro:PBP1-29* (n = 1116), *pid-14/+ 35Spro:PBP1-53* (n = 1889), *pbp1-1* (n = 984), *35Spro:PBP1-29* (n = 595), *35Spro:PBP1-53* (n = 828). *pid-14/+* and *pid-14* indicate lines segregating or homozygous for the *pid-14* allele. Stars (*) indicated that the values are significantly different compared to *pid-14* (Student's t-test, $p < 0.05$).

(D-E) A segregating *pid-14/+* population typically consists of 53 % dicotyledonous seedlings (D) and 47 % tricotyledonous seedlings (E).

(F-I) Seedlings with an aberrant number of cotyledons were observed in *pid-14 pbp1-1*: four cotyledon (F, I), no cotyledon (G) and one cotyledon (H) seedlings.

decrease in *PID* overexpression levels (Figure 2B). Previously, we observed that collapse of the main root meristem is dependent on root growth, as it can only be prevented by exogenous auxin concentrations that completely inhibit root growth (Benjamins et al., 2001). The slight delay in root collapse at four dag by *PBP1* overexpression could thus be explained by the reduction in root growth in the *35Spro:PBP1* lines.

We have indications that PBP1 is a very unstable protein (F. Maraschin, unpublished data). Therefore the level of mRNA overexpression observed by Northern blot analysis may not reflect the actual protein level in the *35Spro:PBP1* seedlings, which would explain this unexpected result. Unfortunately, the above experiments do not permit to draw a clear conclusion concerning the *in planta* function of PBP1 in the PID signaling pathway.

pbp1-1 loss-of-function enhances _pid-14_ embryo phenotypes

A characteristic embryo-based phenotype of *pid* loss-of-function mutants is the aberrant number of cotyledons (mostly three), which is best scored in 5- to 7-day old seedlings and is only observed in part of the homozygous mutant seedlings (Bennett et al., 1995, Christensen et al., 2000, Benjamins et al., 2001). For the *pid-14* allele, an intermediately strong mutant allele caused by a T-DNA insertion in the intron of the *PID* gene, the penetrance of the tricotyledon phenotype is 47 % (n = 1469, Figures 2C and 2E). The influence of modified *PBP1* expression on *pid-14* was investigated by scoring the mutant phenotypes in *pid-14/+ 35Spro:PBP1-53*, *pid-14/+ 35Spro:PBP1-29* and *pid-14/+ pbp1-1* F3 populations.

PBP1 overexpression lead to a mild but significant reduction of the number of tricotyledon seedlings for line *35Spro:PBP1-53* (31 %, n = 1889, Student's t-test, $p < 0.05$, Figure 2C), whereas for line *35Spro:PBP1-29* the reduction was not significant (41 % of tricotyledons, n = 1116, Student's t-test, $p > 0.05$, Figure 2C). This result suggests that PBP1 reduces the severity of the *pid* embryo phenotype, although the decrease of the tricotyledon phenotype penetrance did not correlate with the level of the *PBP1* overexpression.

For the *pid-14/+ pbp1-1* F3 population, the global penetrance of cotyledon defects did not significantly differ from that in *pid-14/+* (43 %, n = 1040, Student's t-test, $p > 0.05$). However, *pbp1-1* loss-of-function did cause a reduction in the penetrance of the tricotyledon phenotype to 32 % (Figure 2C), and instead seedlings were observed with one cotyledon (5 %, Figure 2H), four cotyledons (2 %, Figures 2F and 2I) or even no cotyledon (4 %, Figure 2G). We considered this a significant shift, as tetra-, or nocotyledon seedlings were never observed for the *pid-14* allele, and monocotyledon seedlings only occasionally (0.5 %, n = 1469). Interestingly, *pid-14 pbp1-1* plants produced a few fertile flowers (see below), and this allowed us to reassess the penetrance of the cotyledon in a *pid-14 pbp1-1* double homozygous F4 population. This time, the penetrance of the tricotyledon phenotype

was not significantly changed (45 %, n = 291, Student's t-test, $p > 0.05$, Figure 2C), but on top of that 11 % of the seedlings showed the no-, mono- or tetracotyledon phenotypes as observed in *pid-14/+ pbp1-1*, indicating that *pbp1* loss-of-function does not only change the type of cotyledon defects, but also increases the penetrance of the cotyledon phenotypes. No-, mono- and tetracotyledon seedlings have been reported for some strong *pid* mutant alleles (Bennett et al., 1995), indicating that the absence of *PBP1* expression during embryo development enhances *pid-14* mutant phenotypes, which is in accordance with our conclusions from the *in vitro* kinase assays that PBP1 acts as a positive regulator of PID activity (Benjamins et al., 2003; Galván-Ampudia, unpublished data).

pbp1-1 loss-of-function partially rescues *pid-14* inflorescences

At bolting stage *pid* loss-of-function mutants are characterized by the formation of inflorescence stems with few aberrant flowers and ending in a pin-like structure, thereby mimicking Arabidopsis plants grown on auxin transport inhibitors (Figure 3A) (Okada et al., 1991). The *pid* inflorescence phenotypes are fully penetrant, but may vary in strength depending on the mutant allele. In 5-week old plants of the intermediate strong *pid-14* allele, almost no flowers are observed (Figures 3A and 3D-E). Only 44 % of the inflorescence stems carried flowers, which have the typical *pid* phenotype: fewer stamens and sepals, extra petals and a trumpet-shaped pistil (Figures 3A and 3D, Table 1) (Bennett et al., 1995). Interestingly, in *pid-14 pbp1-1* plants, up to 72 % of the stems carried flowers (Figures 3A-C, Table 1). All these flowers had *pid*-like phenotypes (Figures 3B, 3C, 3I and

Table 1. *pbp1-1* reduces the severity of the *pid-14* pin-like phenotype.

	Stems with flowers[1]	n
Col wild type	100 (0)	10
L*er* wild type	100 (0)	10
35Spro:PBP1-53	100 (0)	10
35Spro:PBP1-29	100 (0)	10
pbp1-1	100 (0)	11
pid-14	44* (19)	10
pid-14 35Spro:PBP1-53	60[!] (21)	7
pid-14 35Spro:PBP1-29	49[!] (28)	5
pid-14 pbp1-1	72[†#] (19)	15

[1] Percentage of stems per five week-old plant with flowers (s.d.)

* Significantly different from Col (Student's t-test, $p < 0.05$)

[†] Significantly different from *pid-14* (Student's t-test, $p < 0.02$)

[!] Significantly different from the respective *35Spro:PBP1* line (Student's t-test, $p < 0.05$)

[#] Significantly different from *pbp1-1* (Student's t-test, $p < 0.02$)

3J). Two kinds of inflorescence were observed in the same plant: wild type-like inflorescence with *pid*-like flowers (Figure 3B) and *pin*-like inflorescences with fewer *pid*-like flowers (Figure 3C). These results suggest that the absence of *PBP1* expression at bolting stage partially rescues the *pid* phenotype, allowing the formation of flowers and the production of few seeds. In contrast, *PBP1* did not have a significant effect on the *pid-14* bolting phenotype (Table 1).

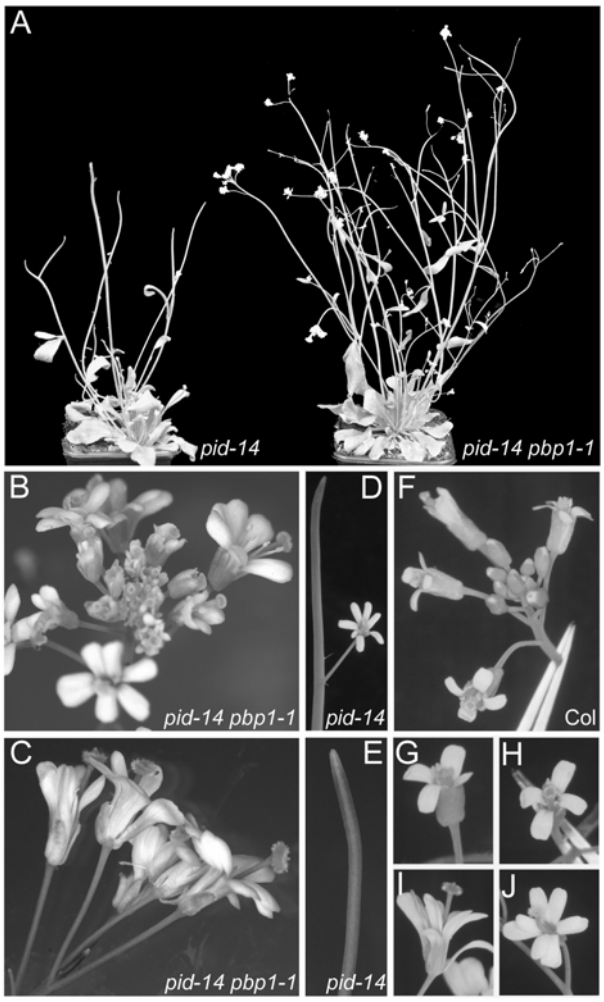

Figure 3. *pbp1-1* loss-of-function partially rescues *pid-14* inflorescences
(A) *pid-14 pbp1-1* plants (right) have a reduced apical dominance compared to *pid-14* (left).
(B, C) *pid-14 pbp1-1* has two types of inflorescences: wild-type with pid-like flowers (B) and pin-like with pid-like flowers (C).
(D, E) *pid-14* has inflorescences with (D) or without (E) flowers.
(F-H) Col wild-type inflorescence (F) has flowers (G, H) with four petals, six stamens and one carpel.
(I, J) *pid-14 pbp1-1* flowers are pid-like with extra number of petals and a trumpet-shaped pistil.

The above results suggest that the effect of PBP1 on PID differs per developmental stage. On the one hand, PBP1 seems to act synergistically with PID during embryo development, as indicated by the enhanced cotyledon defects in *pid-14 pbp1-1* seedlings. On the other hand, PBP1 seems to act antagonistically to PID during inflorescence development, as observed by the partially rescued inflorescences of *pid-14 pbp1-1* plants. The effect of

PBP1 overexpression is minor, and restricted to embryo development, where the observed reduction in the penetrance of cotyledon defects is in line with the proposed synergistic action between PBP1 and PID.

Auxin-induced sequestration of PID to the cytoplasm is PBP1-independent

To further analyze the effect of the PBP1-dependent regulation of PID in plants, we analyzed whether *PBP1* overexpression had any effect on PID expression and localization using the *PIDpro:PID:VENUS* marker line (Michniewicz et al., 2007). For this we focused our attention to epidermal cells in the distal elongation zone, as *PID* is expressed in this region (Michniewicz et al., 2007), and *PBP1* overexpression resulted in a significant reduction in root length.

PID is a plasma membrane-associated kinase (Figure 4A) (Lee and Cho, 2006, Michniewicz et al., 2007). Previously, we observed that PID localization is highly dynamic, and that auxin treatment induces its rapid and transient sequestration from the plasma membrane to the cytoplasm (Figure 4E and Chapter 2, this thesis). The auxin-dependent release of PID from the plasma membrane seems to rely on an increase of the cytoplasmic calcium concentration through plasma membrane calcium channels, and on calmodulin-like activity, as it can be inhibited by pre-incubation with the plasma membrane calcium channel inhibitor Tetracain (Figure 4G), or with the calmodulin inhibitor Lanthanum (Figure 4H). *PBP1* overexpression did not result in a clear alteration of PID localization (Figure 4B), but it did partially inhibit the transient sequestration of PID (Figure 4F). These results suggest that PBP1 itself is not involved in the auxin-induced sequestration of PID in root epidermal cells, but that instead its overexpression stabilizes the membrane association of PID.

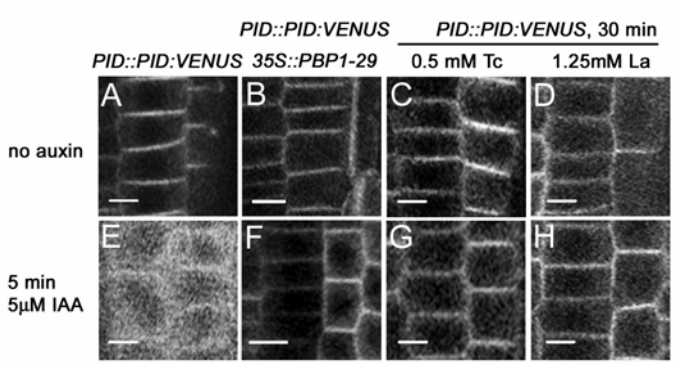

Figure 4. PBP1 stabilizes the plasma membrane association of PID.
(A-H) Confocal sections showing the subcellular localization of PID:VENUS in epidermal cells of the elongation zone of seedling root tips of the lines *PIDpro:PID:VENUS* (A, C-E, G, H) and *PIDpro:PID:VENUS 35Spro:PBP1-29* (B, F). PID is membrane localized in control medium (A, B), but is transiently sequestered to the cytoplasm after 5 min treatment with 5 μM IAA (E), but less when PBP1 is overexpressed (F). A 30 min pre-

treatment with 0.5 mM Tetracain (C, G) or 1.25 mM Lanthanum (D, H) did not affect PID localization, but blocked the auxin-induced transient sequestration to the cytosol (G, H). Scale bars represent 10 µm.

PBP1H acts redundantly with its close homolog PBP1 to positively regulate PID activity

PBP1 and PBP1H are highly conserved with 80 % amino acid sequence identity (Figure 5A), and pull down experiments indicated that PID also interacts with PBP1H (C. Galván-Ampudia, unpublished data). Since the loss-of-function allele *pbp1-1* did not give phenotypes, other than the increased root length, we suspected that the two proteins were functionally redundant, and tried to identify *pbp1h* loss-of-function alleles. Unfortunately, in the two available T-DNA insertion lines (SALK_013868 and SALK_048098) with T-DNAs at positions -673 and -582 relative to the *PBP1H* ATG, respectively, *PBP1H* expression was found to be at wild type levels (data not shown). Therefore, we attempted to knock-down both *PBP1* and *PBP1H* expression through RNA interference (RNAi), by overexpressing a hairpin RNA spanning the complete *PBP1H* coding region (*hpPBP1H*). Several lines were obtained containing a single locus insertion of the *hpPBP1H* construct, two of which (*hpPBP1H-13* and *hpPBP1H-16*) were studied in more detail. Expression analysis showed that *PBP1H* expression in both lines was significantly reduced (Figure 5B). The residual fragment amplified in both lines was also observed in the minus reverse transcriptase control, indicating that it was derived from contaminating DNA. In the *hpPBP1H-13* sample, a larger additional band was detected. Since Northern blot analysis indicated that line *hpPBP1H-13* shows the highest expression of the *hpPBP1H* RNA (results not shown), it is likely that this fragment represents the full length hairpin RNA amplified with the forward PCR primer. As anticipated based on the homology between the *PBP1* and *PBP1H* coding regions (78 % identity), *PBP1* expression was also suppressed in *hpPBP1H-13* and was even undetectable in *hpPBP1H-16* (Figure 5B).

Figure 5. (continued)

(C) The percentage of main root growth in L*er* wild type, *pbp1-1*, *hpPBP1H-13* and *hpPBP1H-16* seedlings, normalized to Col wild type seedlings. The mean of three experiments is shown. Stars (*) and hash signs (#) indicate significant differences compared to Col and L*er*, respectively (Student's t-test, $p < 0.06$).

(D) The percentage of main root meristem collapse in *35Spro:PID-21*, *35Spro:PID-21 hpPBP1H-13* and *35Spro:PID-21 hpPBP1H-16* seedlings at 3, 4, and 5 days after germination (dag).

(E) The percentage of seedling phenotypes in *pid-14/+, pid-14/+ hpPBP1H-13, pid-14/+ hpPBP1H-16, pid-14/+ pbp1-1 hpPBP1H-16, hpPBP1H-13* and *hpPBP1H-16. pid-14/+* and *pid-14* indicate lines segregating or homozygous for the *pid-14* allele, respectively. Stars (*) indicate significant differences compared to *pid-14* (Student's t-test, $p < 0.06$).

(F-G) Seedling phenotypes observed in progeny of *pid-14/+*: a normal dicotyledonous seedling (F) and a tricotyledonous seedling (G) observed in 45% of the individuals homozygous for the *pid-14* loss-of-function mutation.

(H-J) Seedlings with four cotyledons (H), one cotyledon (I) and no cotyledon (J), as observed among progeny of the lines *pid-14/+ hpPBP1H-13, pid-14/+ hpPBP1H-16* and *pid-14/+ pbp1-1 hpPBP1H-16*.

(K-M) Seedlings without hypocotyl (K), without hypocotyl and root (L) and with fused cotyledons are found in *pid-14 hpPBP1H-13, pid-14 hpPBP1H-16* and *pid-14 pbp1-1 hpPBP1H-16* (M).

(N-O) Seedlings without cotyledons in *pid-14 pbp1-1 hpPBP1H-16* show defects in the phyllotaxis of the first leaves, with either fused leaves (N) or fused petioles (O).

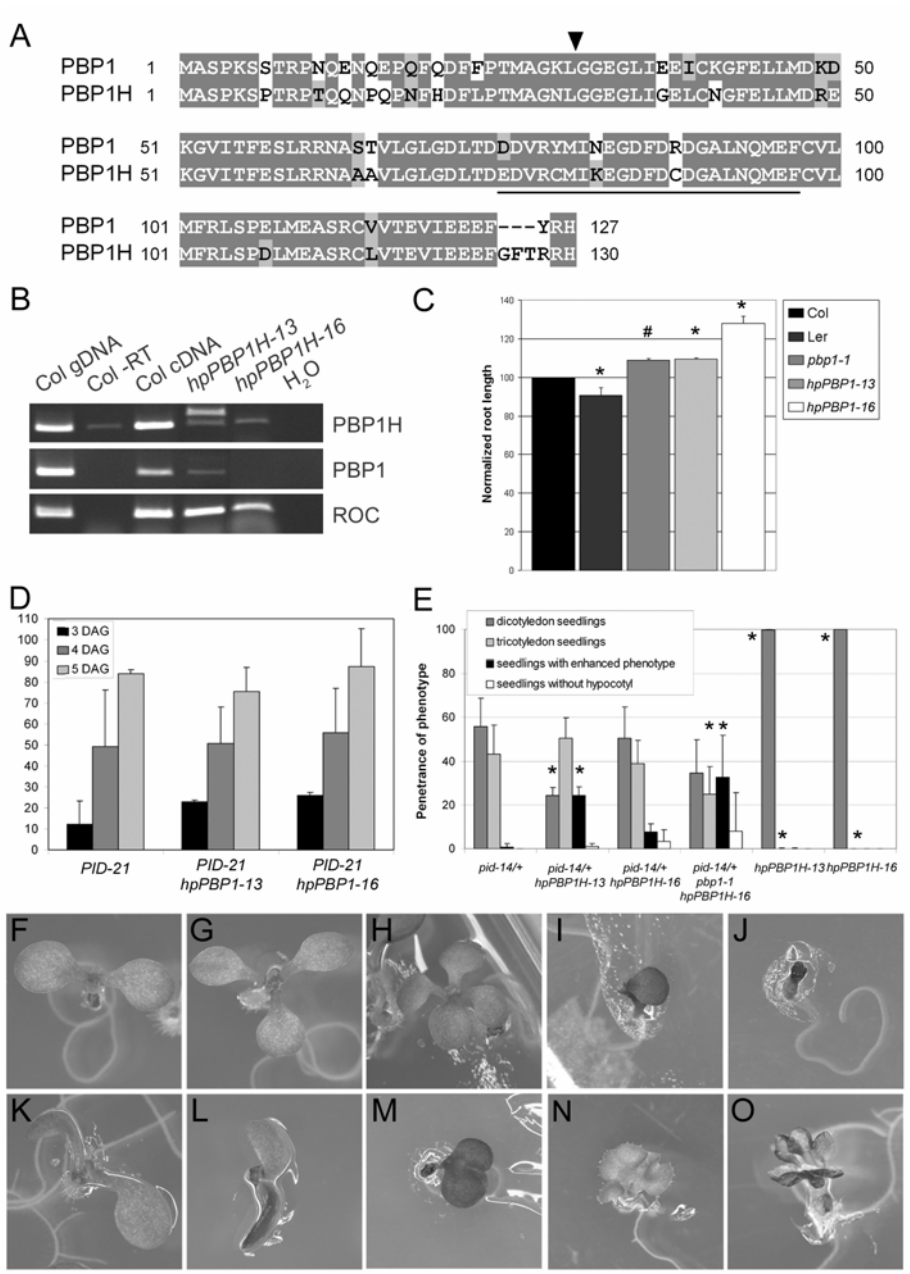

Figure 5. PBP1 and PBP1H act redundantly on root growth, embryo patterning and leaf phyllotaxis.
(A) Alignment of the PBP1 and PBP1H proteins. The arrowhead indicates the position of the transposon insertion in *pbp1-1*. The EF-hand domain is underlined.

(B) RT-PCR reactions showing that both *PBP1* (middle) and *PBP1H* (top) expression are reduced in *hpPBP1H-13* whereas *PBP1* expression is absent in *hpPBP1H-16.* Controls are Col genomic DNA (gDNA), Col RNA in which the reverse transcriptase was omitted during the RT reaction (Col -RT), Col cDNA and water.

Overall, *hpPBP1H-13* and *hpPBP1H-16* plants had a wild type phenotype, but similar to *pbp1-1*, the primary seedling roots were longer compared to the wild type control (109 % and 128 %, respectively, Student's t-test, $p < 0.06$, Figure 5C). Interestingly, the increase in root length correlated with the level of *PBP1* knock-down in these lines.

To further investigate the function of PBP1H in the PID pathway, the *hpPBP1H* lines were crossed with *35Spro:PID-21,* and the main root meristem collapse was analyzed in the progeny of double homozygous F2 plants. Similar to the *pbp1-1* loss-of-function allele, the *hpPBP1H*-induced knock-down of both *PBP1* and *PBP1H* did not significantly influence the root collapse kinetics of *PID* overexpression (Student's t-test, $p > 0.05$, Figure 5D).

In addition, we crossed *hpPBP1H* lines with the *pid-14* allele, and counted the number of seedlings with aberrant cotyledon phenotypes in progeny of *pid-14/+ hpPBP1H* F2 plants. A greater number of seedlings with cotyledon defects could be observed in *pid-14/+ hpPBP1H-13* (even up to 75 %) and *pid-14/+ hpPBP1H-16* compared to *pid-14/+* and *pid-14/+ pbp1-1* (Figures 5E and 5H-J). In both *pid-14/+ hpPBP1H-13* and *pid-14/+ hpPBP1H-16* the number of monocotyledon seedlings was increased (8 % and 6 %, respectively, Figure 5I), whereas a significant number of seedlings without cotyledon could be observed in *pid-14/+ hpPBP1H-13 (*15 %, Figure 5J). Furthermore, several seedlings without hypocotyl (Figure 5K) or without hypocotyl and root (Figure 5L) were observed in *pid-14/+ hpPBP1H-16* (> 3 %, Figure 5E), indicating that PID, PBP1, PBP1H are involved in broader aspects of embryo patterning than only cotyledon initiation and positioning.

To corroborate these data, we generated *pid-14/+ pbp1-1 hpPBP1H-16* triple lines, homozygous for *pbp1-1* and *hpPBP1H-16*, and heterozygous for *pid-14*, and scored for cotyledon defects in the progeny. The severity of the embryo/seedling phenotypes was enhanced compared to the two *pid-14 hpPBP1H* and the *pid-14 pbp1-1* lines, with 32 % of seedlings showing enhanced seedling phenotype (Figures 5E and 5H-O). The majority of these seedlings had one (14 %, Figure 5I) or no cotyledon (18 %, Figure 5J), and the number of seedlings without hypocotyl or without hypocotyl and root was increased to 8 % (Figure 5K and 5L). Furthermore, monocotyledon seedlings had defects in the formation of the first leaves, which were fused at the blade (Figure 5N) or at the petiole (Figure 5O). Normal plant growth and organ positioning were restored for the subsequent leaves. These data suggest that PBP1 and PBP1H act redundantly in the PID pathway and have a positive effect on the kinase function. Defects in embryo patterning and leaf phyllotaxis in *pid-14 pbp1-1 hpPBP1H-16* confirms the proposed role of PID in regulation of organ boundaries during embryogenesis (Furutani et al., 2004).

Discussion

The plant signaling molecule auxin controls plant development through transport-generated auxin gradients. Previous experiments have indicated that calcium is an important second messenger in auxin action. One of the earliest cellular responses to auxin is a rapid increase in cytosolic calcium (Felle, 1988, Gehring et al., 1990, Shishova and Lindberg, 2004) and calcium has been reported to play a crucial role in PAT (Dela Fuente and Leopold, 1973). The direction of PAT is determined by the asymmetrical subcellular localization of the PIN auxin efflux carriers (Wisniewska et al., 2006). The protein kinase PID has been shown to direct the polar targeting of PIN proteins by phosphorylation of residues in their large central hydrophilic loop (Friml et al., 2004, Michniewicz et al., 2007). The finding that PID interacts in a calcium-dependent manner with the calmodulin-like protein TCH3 and the small calcium-binding protein PBP1, provided the first molecular evidence for the role of calcium as regulator of PAT (Benjamins et al., 2003). In this chapter, we further investigated the role of PBP1 in plant development in relation to its interaction with PID.

PBP1(H) regulates root growth by enhancing PID activity

PBP1 belongs to a small family of single EF-hand calcium-binding proteins (Reddy et al., 2004), and was found to enhance the PID kinase activity in *in vitro* phosphorylation assays (Benjamins et al., 2003; Chapter 2, this thesis). To analyze the *in planta* role of PBP1 in the PID pathway, we isolated loss- and gain-of function mutants in the *PBP1* gene and its close homologue *PBP1H*. Morphometric analysis of these mutant lines indicated that PBP1 and PBP1H are partially redundant to repress root growth, and although we could not find clear evidence for a change in sensitivity of the mutant lines to auxin, PAT inhibitors or *PID* overexpression, it is likely that PBP1 and PBP1H mediate their effect on root growth through their role as positive regulators of PID activity. PID overexpression may lead to increased auxin transport to the root elongation zone (Benjamins et al., 2001, Friml et al., 2004, Lee and Cho, 2006), which in turn inhibits root growth and thus explains the longer root in *pbp1(h)* loss-of-function lines and the shorter root in *PBP1* overexpression lines. This positive regulatory function of PBP1(H) in PID pathway in roots is similarly observed during embryogenesis by the enhanced penetrance and/or severity of seedling phenotypes in *pid-14 pbp1-1*, *pid-14 hpPBP1H*, *pid-14 pbp1-1 hpPBP1H-16* mutant lines as compared to *pid-14*.

In chapter 2, we showed auxin-induced and calcium-dependent sequestration of PID in epidermis cells of the root elongation zone. Here we present data that this occurs independent of PBP1, and that, in fact *PBP1* overexpression even enhances the membrane-

association of PID. On the one hand, these results corroborate our model that TCH3 is involved in PID sequestration, and on the other hand, it shows that PBP1 not only positively regulates PID action by enhancing its kinase activity, but also by retaining the kinase at the plasma membrane, in proximity of its phosphorylation targets, the PIN proteins.

PBP1(H) assists PID in establishing organ boundaries during embryogenesis

Upon germination, seedlings have a bilateral symmetry marked by the presence of two cotyledons separated by the shoot-root axis. This symmetric structure can be traced back to the early embryogenesis, when the initiation of cotyledon primordia in the globular embryo marks the transition to the heart stage. Proper auxin distribution, based on the PAT activity, is primordial for the embryo patterning at crucial transition steps (Friml et al., 2003, Weijers et al., 2005, Weijers and Jürgens, 2005). The auxin efflux carriers PIN1, PIN3, PIN4 and PIN7 are involved in controlling the auxin gradients during embryogenesis (Friml et al., 2003). At heart stage, the establishment of the cotyledons boundaries is based on the presence of an auxin maximum at the cotyledon tips. Treatment of embryos with exogenous auxin or PAT inhibitors gives rise to seedlings with abnormally positioned or fused cotyledons (Friml et al., 2003, Furutani et al., 2004). And mutations in *PIN1* and *PID* generate seedlings with an abnormal number of cotyledons. The *pin1 pid* double mutant seedlings have no cotyledons and fused leaves with an aberrant phyllotaxis. Both proteins, by controlling auxin distribution, are responsible for the establishment of a bilateral symmetry and the cotyledon outgrowth during embryogenesis (Furutani et al., 2004). We have observed that in the *pid-14* mutant background the absence of the PID positive regulators PBP1 and PBP1H perturbed embryogenesis even more, giving rise to seedlings with no to four cotyledons, whereas only tricotyledon seedlings were observed in *pid-14*. Such phenotypes were previously described for strong alleles of *pid* or in the combination of *pid* with the *enhancer of pid* mutation (Bennett et al., 1995, Treml et al., 2005). Together these results confirm the proposed role of PID in the regulation of organ boundaries establishment (Furutani et al., 2004) and the function of PBP1 and PBP1H as positive regulator of PID kinase activity during embryogenesis and seedling development.

In *pid-14 hpPBP1H-16* and *pid-14 pbp1-1 hpPBP1H-16*, seedlings with strong patterning defects such as absence of hypocotyl or both hypocotyl and root were observed at low frequencies. Similar phenotypes have been reported for mutants impaired in auxin transport and signaling during embryogenesis like *pin1 pin3 pin4 pin7* quadruple mutant, *gnom*, *monopteros* and *bodenlos* (Friml et al., 2003). In these mutants, miss-specification of the embryonic hypophysis leads to an absence of the root pole. This reveals the importance of auxin transport and signaling for proper embryo patterning and the establishment of the shoot-root axis. It is therefore likely that PID is not only involved in cotyledon positioning,

but also in the establishment/maintenance of the shoot-root axis by regulating the highly dynamic and regulated auxin transport during embryo development.

Phyllotaxis regulation by PID activity

The regular arrangement of leaves and flowers around the stem, so-called phyllotaxis, is also a highly auxin-dependent regulated mechanism (Reinhardt et al., 2003). Besides the cotyledon defects during embryo development, *pin1* and *pid* loss-of-function mutants are both defective in aerial organ formation during their adult phase, which is characterized by oddly positioned and shaped leaves and pin-like inflorescences carrying a few aberrant flowers. Interestingly, *pin1* and *pid* loss-of-function mutants react differently to auxin application at the tip of their pin-like inflorescences. In *pin1* mutants, auxin treatment generates the formation of a ring-shape primordium, indicating that PIN1 plays a crucial role in organ separation in the inflorescence meristem as was observed in seedlings. In *pid* mutants, an auxin dose-dependent number of normal sized flowers were induced, suggesting that the mechanism of auxin transport is still present and functional in *pid*, and that the inflorescence meristem retains part of its patterning capacity (Reinhardt et al., 2003). In *pid-14 pbp1-1*, partial rescue of the *pid-14* pin-like structure by *pbp1-1* was observed with the formation of *pid*-like flowers, mimicking auxin application at the inflorescence meristem (Reinhardt et al., 2003). Such phenotypes as well as the formation of functional shoot apical meristems in *pid-14 pbp1-1* are also observed in weak *pid* alleles (Bennett et al., 1995).

Although an enhancement of the *pid* phenotype by *pbp1* or by *pbp1h* was anticipated, the partial rescue of the *pid* inflorescence phenotypes in the *pid-14 pbp1-1* double mutant suggests that PIN1, basal localized in epidermal cells in *pid* inflorescence meristem (Friml et al., 2004), may be restored at its normal, apical, subcellular localization in *pid-14 pbp1-1*, resulting in a normal auxin distribution in the inflorescence meristem and an induction of the flower formation. These results and previous observations suggest that PID may not be involved in the formation of primordia boundaries in the inflorescence meristem, as it does during embryogenesis, since a phyllotactic pattern can be observed upon auxin application (Reinhardt et al., 2003) or in absence of its positive regulators (this work). One has to keep in mind, however, that PID is a member of the AGCVIII family of protein kinases, and that in Arabidopsis it groups together in the AGC3 clade that comprises three PID-related kinases (PRKs) (Galván-Ampudia and Offringa, 2007). We are currently investigating the possibility that these other kinases act redundantly with PID in inflorescence development, and if this is the case, whether the expression of one of these kinases is up-regulated in the *pid-14 pbp1-1* double mutant and not in *pid-14*. Interestingly, the rescue of *pid-14* phenotype observed in *pid-14 pbp1-1* plants is not presented anymore

in the *pid-14 wag1 wag2 pbp1-1* quadruple mutant, suggesting that this is indeed the case (Galván-Ampudia et al., manuscript in preparation).

Materials and methods

Plasmids and molecular cloning

Molecular cloning was performed following standard procedures (Sambrook et al., 1989). Bacteria were grown on LC medium containing 100 µg/ml carbenicillin (Cb) for *E. coli* strains DH5α or Rosetta (Novagen), 50 µg/ml kanamycin (Km) or 250 µg/ml spectinomycin for respectively binary vectors pCAMBIA1300 and pART27 in *E. coli* DH5α or *Agrobacterium tumefaciens* strain LBA1115. For the latter strain, 20 µg/ml rifampicin was included in the LC medium.

The construct pSDM6015 (pBS-SK-PBP1) was previously described (Benjamins et al., 2003). For the *35Spro:PBP1* construct, the *PBP1* cDNA was excised as a *Sal*I-*Spe*I fragment from pSDM6015 and cloned into pCambia1300int-35Snos, given rise to pSDM6085. To obtain the *PBP1H* RNAi construct, a *PBP1H* fragment was PCR amplified from pET-PBP1H (pSDM6042) using the primers 5'TC-*Eco*RI-ATGGCGTCACCAAAGTCACC3' and 5'CAAATCTCTCCAGTG-*Kpn*I-ATGC3', and ligated as anti-sense *Eco*RI-*Kpn*I fragment into the pHANNIBAL vector (Wesley et al., 2001). The sense fragment was excised as a *Cla*I-*Bam*HI fragment from pET-PBP1H and cloned into the corresponding restriction sites in pHANNIBAL. The resulting *PBP1H* RNAi expression cassette (pSDM6043) was transferred to the pART27 binary vector as a *Not*I fragment (pSDM6302).

Arabidopsis lines, plant growth and transformation

The *35Spro:PID-21* (Benjamins et al., 2001) and the *PIDpro:PID:VENUS* (Michniewicz et al., 2007) lines were described previously. The *pid-14* (SALK_049736), *pbp1-1* (Ds transposon line GT6553) and *pbp1h-1* and *-2* alleles (SALK_013868 and SALK_048098) were obtained from NASC for the SALK lines (Alonso et al., 2003) and from the Cold Spring Harbor Laboratory for the transposon insertion line (Sundaresan et al., 1995). For the detection of the insertions, we used gene-specific primers 5'TCTCTTCCGCCAGGTAAAAA3' and 5'CGCAAGACTCGTTGGAAAAG3' for *PID*, 5'TACCCTTACGTGAGCTTCCAA3' and 5'TCACCTCCGTCACAACACAC3' for *PBP1*, 5'CATGCAATTAGAGAACGGGCA3' and 5'AGGAACATCCATGGAAGCCA3' for *PBP1H* and the insertion-specific primers LBaI and Ds3-2 for respectively the SALK lines and the transposon line. The flanking region of each insertion was sequenced to

confirm the insertion position and RT-PCR analysis was performed to determine if the insertion resulted in a complete loss-of-function allele.

Arabidopsis seeds were surfaced-sterilized by incubation for 15 min in 50 % commercial bleach solution and rinsed four times with sterile water. Seeds were vernalized for 2 to 4 days at 4°C and germinated (21°C, 16 h-photoperiod and 3000 lux) on solid MA medium (Masson and Paszkowski, 1992) supplemented with antibiotics when required. Two- to three-week old plants were transferred to soil and grown at 21°C and 70 % relative humidity with a 16 h photoperiod of 10000 lux.

Arabidopsis thaliana ecotype Columbia (Col) was transformed by the floral dip method as described (Clough and Bent, 1998). Primary transformants were selected on medium supplemented with 20 µg/ml hygromycin (Hm) for pSDM6085 or 70 µg/ml Km for pSDM6302 and 100 µg/ml timentin to inhibit the Agrobacterium growth. For further analysis, single locus insertion lines were selected by germination on 10 µg/ml Hm or 25 µg/ml Km and checked for transgene expression by Northern blot or RT-PCR analysis.

Northern blot and RT-PCR analysis

Total RNA was purified using the RNeasy Plant (Qiagen) and Invisorb Spin Plant RNA (Invitek) Mini kits. Subsequent RNA blot analysis was performed as described (Memelink et al., 1994) using 10 µg of total RNA per sample. The following modifications were made: pre-hybridizations and hybridizations were conducted at 65°C using 10 % Dextran sulfate, 1 % SDS, 1 M NaCl, 50 µg/ml of single strand Herring sperm DNA as hybridization mix. The hybridized blots were washed for 20 min at 65°C in 2x SSPE 0.5 % SDS, and for 20 min at 42°C in respectively 0.2x SSPE 0.5 % SDS, 0.1x SSPE 0.5 % SDS and 0.1x SSPE. Blots were exposed to X-ray film FUJI Super RX. Probes were PCR amplified and column purified (Qiagen): 5'CCTCAACAAGACCAAACCAAG3', 5'TCACCTCCGTCACAACACAC3' for *PBP1* from pSDM6007; 5'ATGGCGTCACCAAAGTCACC3', 5'TGTTCAACACATCTGATCAAAGA3' for *PBP1H*, 5'AGGCACGTGACAACGTCTC3', 5'CGCAAGACTCGTTGGAAAAG3' for *PID*, 5'CGGGAAGGATCGTGATGGA3', 5CCAACCTTCTCGATGGCCT3' for *AtROC5*, 5'CGGAATTCATGAGAGAGATCCTTCATATC3', 5'CCCTCGAGTTAAGTCTCGTACTCCTCTTC3' for *αTubulin* from Col genomic DNA. Probes were radioactively labeled using α-^{32}P-ATP (Amersham) and the Prime-a-gene kit (Promega).

RT-PCRs were performed as described (Weijers et al., 2001) using 10 µg of total RNA from one-week old seedlings for the RT reaction. The PCR reactions were performed with one tenth of the RT volume with the same gene specific primers used for the probe amplification in the Northern blot analysis. A RT reaction from Col seedlings RNA in which the reverse-transcriptase was omitted served as a negative control.

Biological assays

For the root meristem collapse assay, about 100 seedlings per line were grown in triplicate on vertical plates containing solid MA medium. The development of the seedling root was monitored and scored each day during eight days for the collapse of the primary root meristem. For the phenotypic analysis of the crosses with *pid-14*, about 300 seeds (100 seeds for *pid-14 pbp1-1* and controls) were plated in triplicate, germinated and grown for one week on solid MA medium. The number of dicotyledon seedlings and of seedlings with cotyledon defects was counted and the penetrance of the phenotypes was calculated based on a 1:3 segregation ratio for homozygous *pid/pid* seedlings. For root length measurements, at least 50 seedlings for each genotype were grown in triplicate on vertical plate for eight days and roots were photographed. Root lengths were measured using ImageJ (http://rsb.info.nih.gov/ij/). To observe the auxin-induced changes in the subcellular localization of PID in Arabidopsis roots, vertically grown three day-old *PIDpro:PID:VENUS* and *PIDpro:PID:VENUS 35Spro:PBP1-29* seedlings were treated with 5 µM IAA (in MA medium) following 30 min pre-treatment with a calmodulin inhibitor (0.5 mM Tetracain, Sigma) or a calcium channel blocker (1.25 mM Lanthanum, Sigma).

Confocal microscopy

Arabidopsis *PIDpro:PID:VENUS* roots were observed using a 40x oil objective with a ZEISS Axioplan microscope equipped with a confocal laser scanning unit (MRC1024ES, BioRad, Hercules, CA). The YFP fluorescence was monitored with a 522-532 nm band pass emission filter (488 nm excitation). All images were recorded using a 3CCD Sony DKC5000 digital camera. The images were processed by ImageJ and assembled in Adobe Photoshop 7.0.

Accession Numbers

The *Arabidopsis* Genome Initiative locus identifiers for the genes mentioned in this chapter are as follows: *PBP1/KRP2* (At5g54490), *PBP1H/KRP1* (At4g27280), *KIC* (At2g46600), *PID* (At2g34650), *TCH3* (At2g41100), *KCBP* (At5g65930), *KIPK* (At3g52890), *ROC* (At4g38740), *αTubulin* (At5g44340).

Acknowledgments

The authors thank Carlos Galván-Ampudia for valuable discussions and critical reading, Marcus Heisler and Pieter Ouwerkerk for kindly providing the *PIDpro:PID:VENUS* line

and pCambia1300int-35Snos, respectively, and Gerda Lamers and Ward de Winter for their help with the microscopy and the tissue culture, respectively

References

Alonso,J.M., Stepanova,A.N., Leisse,T.J., Kim,C.J., Chen,H., Shinn,P., Stevenson,D.K., Zimmerman,J., Barajas,P., Cheuk,R., Gadrinab,C., Heller,C., Jeske,A., Koesema,E., Meyers,C.C., Parker,H., Prednis,L., Ansari,Y., Choy,N., Deen,H., Geralt,M., Hazari,N., Hom,E., Karnes,M., Mulholland,C., Ndubaku,R., Schmidt,I., Guzman,P., Aguilar-Henonin,L., Schmid,M., Weigel,D., Carter,D.E., Marchand,T., Risseeuw,E., Brogden,D., Zeko,A., Crosby,W.L., Berry,C.C., and Ecker,J.R. (2003). Genome-Wide Insertional Mutagenesis of Arabidopsis thaliana. Science **301**:653-657.

Benjamins,R., Galván-Ampudia,C.S., Hooykaas,P.J., and Offringa,R. (2003). PINOID-mediated signaling involves calcium-binding proteins. Plant Physiol **132**:1623-1630.

Benjamins,R., Quint,A., Weijers,D., Hooykaas,P., and Offringa,R. (2001). The PINOID protein kinase regulates organ development in Arabidopsis by enhancing polar auxin transport. Development **128**:4057-4067.

Benková,E., Michniewicz,M., Sauer,M., Teichmann,T., Seifertová,D., Jürgens,G., and Friml,J. (2003). Local, efflux-dependent auxin gradients as a common module for plant organ formation. Cell **115**:591-602.

Bennett,S.R.M., Alvarez,J., Bossinger,G., and Smyth,D.R. (1995). Morphogenesis in Pinoid Mutants of Arabidopsis-Thaliana. Plant Journal **8**:505-520.

Christensen,S.K., Dagenais,N., Chory,J., and Weigel,D. (2000). Regulation of auxin response by the protein kinase PINOID. Cell **100**:469-478.

Clough,S.J. and Bent,A.F. (1998). Floral dip: a simplified method forAgrobacterium-mediated transformation ofArabidopsis thaliana. The Plant Journal **16**:735-743.

Day,I.S., Miller,C., Golovkin,M., and Reddy,A.S. (2000). Interaction of a kinesin-like calmodulin-binding protein with a protein kinase. J.Biol.Chem. **275**:13737-13745.

Dela Fuente,R.K. and Leopold,A.C. (1973). A Role for Calcium in Auxin Transport. Plant Physiol **51**:845-847.

Felle,H. (1988). Auxin causes oscillations of cytosolic free calcium and pH in Zea mays coleoptiles. Planta **V174**:495-499.

Friml,J., Yang,X., Michniewicz,M., Weijers,D., Quint,A., Tietz,O., Benjamins,R., Ouwerkerk,P.B.F., Ljung,K., Sandberg,G., Hooykaas,P.J.J., Palme,K., and Offringa,R. (2004). A PINOID-dependent binary switch in apical-basal PIN polar targeting directs auxin efflux. Science **306**:862-865.

Friml,J., Vieten,A., Sauer,M., Weijers,D., Schwarz,H., Hamann,T., Offringa,R., and Jurgens,G. (2003). Efflux-dependent auxin gradients establish the apical-basal axis of Arabidopsis. Nature **426**:147-153.

Friml,J., Wisniewska,J., Benková,E., Mendgen,K., and Palme,K. (2002). Lateral relocation of auxin efflux regulator PIN3 mediates tropism in Arabidopsis. Nature **415**:806-809.

Furutani,M., Vernoux,T., Traas,J., Kato,T., Tasaka,M., and Aida,M. (2004). PIN-FORMED1 and PINOID regulate boundary formation and cotyledon development in Arabidopsis embryogenesis. Development **131**:5021-5030.

Galván-Ampudia,C.S. and Offringa,R. (2007). Plant evolution: AGC kinases tell the auxin tale. Trends Plant Sci. **12**.

Gehring,C.A., Irving,H.R., and Parish,R.W. (1990). Effects of auxin and abscisic acid on cytosolic calcium and pH in plant cells. Proc.Natl.Acad.Sci.U.S.A **87**:9645-9649.

Lee,S.H. and Cho,H.T. (2006). PINOID Positively Regulates Auxin Efflux in Arabidopsis Root Hair Cells and Tobacco Cells. Plant Cell **18**:1604-1616.

Masson,J. and Paszkowski,J. (1992). The Culture Response of Arabidopsis-Thaliana Protoplasts Is Determined by the Growth-Conditions of Donor Plants. Plant Journal **2**:829-833.

Memelink,J., Swords,K.M.M., Staehelin,L.A., and Hoge,J.H.C. (1994) Southern, Northern and Western blot analysis. In Plant Molecular Biology Manuel, (Dordrecht, NL: Kluwer Academic Publishers).

Michniewicz,M., Zago,M.K., Abas,L., Weijers,D., Schweighofer,A., Meskiene,I., Heisler,M.G., Ohno,C., Huang,F., Weigel,D., Meyerowitz,E.M., Luschnig,C., Offringa,R., and Friml,J. (2007). Phosphatase 2A and PID kinase activities antagonistically mediate PIN phosphorylation and apical/basal targeting in *Arabidopsis*. Cell **130**:1044-1056.

Okada,K., Ueda,J., Komaki,M.K., Bell,C.J., and Shimura,Y. (1991). Requirement of the Auxin Polar Transport System in Early Stages of Arabidopsis Floral Bud Formation. Plant Cell **3**:677-684.

Petrášek,J., Mravec,J., Bouchard,R., Blakeslee,J.J., Abas,M., Seifertová,D., Wisniewska,J., Tadele,Z., Kubes,M., Covanová,M., Dhonukshe,P., Skupa,P., Benková,E., Perry,L., Krecek,P., Lee,O.R., Fink,G.R., Geisler,M., Murphy,A.S., Luschnig,C., Zazimalova,E., and Friml,J. (2006). PIN Proteins Perform a Rate-Limiting Function in Cellular Auxin Efflux. Science **312**:914-918.

Reddy,A.S. and Day,I.S. (2000). The role of the cytoskeleton and a molecular motor in trichome morphogenesis. Trends Plant Sci. **5**:503-505.

Reddy,V.S., Day,I.S., Thomas,T., and Reddy,A.S. (2004). KIC, a novel Ca2+ binding protein with one EF-hand motif, interacts with a microtubule motor protein and regulates trichome morphogenesis. Plant Cell **16**:185-200.

Reinhardt,D., Pesce,E.R., Stieger,P., Mandel,T., Baltensperger,K., Bennett,M., Traas,J., Friml,J., and Kuhlemeier,C. (2003). Regulation of phyllotaxis by polar auxin transport. Nature **426**:255-260.

Sabatini,S., Beis,D., Wolkenfelt,H., Murfett,J., Guilfoyle,T., Malamy,J., Benfey,P., Leyser,O., Bechtold,N., Weisbeek,P., and Scheres,B. (1999). An auxin-dependent distal organizer of pattern and polarity in the Arabidopsis root. Cell **99**:463-472.

Sambrook,J., Fritsch F., and Maniatis,T. (1989) Molecular cloning - A laboratory Manual. C.Nolan, ed Cold Spring Harbor Laboratory press, NY, USA).

Shishova,M. and Lindberg,S. (2004). Auxin induces an increase of Ca2+ concentration in the cytosol of wheat leaf protoplasts. J Plant Physiol **161**:937-945.

Sundaresan,V., Springer,P., Volpe,T., Haward,S., Jones,J.D., Dean,C., Ma,H., and Martienssen,R. (1995). Patterns of gene action in plant development revealed by enhancer trap and gene trap transposable elements. Genes and Development **9**:1797-1810.

Tanaka,H., Dhonukshe,P., Brewer,P.B., and Friml,J. (2006). Spatiotemporal asymmetric auxin distribution: a means to coordinate plant development. Cell Mol.Life Sci. **63**:2738-2754.

Treml,B.S., Winderl,S., Radykewicz,R., Herz,M., Schweizer,G., Hutzler,P., Glawischnig,E., and Ruiz,R.A.T. (2005). The gene ENHANCER OF PINOID controls cotyledon development in the Arabidopsis embryo. Development **132**:4063-4074.

Weijers,D. and Jürgens,G. (2005). Auxin and embryo axis formation: the ends in sight? Curr.Opin.Plant Biol. **8**:32-37.

Weijers,D., Sauer,M., Meurette,O., Friml,J., Ljung,K., Sandberg,G., Hooykaas,P., and Offringa,R. (2005). Maintenance of embryonic auxin distribution for apical-basal patterning by PIN-FORMED-dependent auxin transport in Arabidopsis. Plant Cell **17**:2517-2526.

Weijers,D., Franke-van Dijk,M., Vencken,R.J., Quint,A., Hooykaas,P., and Offringa,R. (2001). An Arabidopsis Minute-like phenotype caused by a semi-dominant mutation in a RIBOSOMAL PROTEIN S5 gene. Development **128**:4289-4299.

Wesley,S.V., Helliwell,C.A., Smith,N.A., Wang,M., Rouse,D.T., Liu,Q., Gooding,P.S., Singh,S.P., Abbott,D., Stoutjesdijk,P.A., Robinson,S.P., Gleave,A.P., Green,A.G., and Waterhouse,P.M. (2001). Construct design for efficient, effective and high-throughput gene silencing in plants. The Plant Journal **27**:581-590.

Wisniewska,J., Xu,J., Seifertová,D., Brewer,P.B., Ruzicka,K., Blilou,I., Rouquié,D., Benková,E., Scheres,B., and Friml,J. (2006). Polar PIN localization directs auxin flow in plants. Science **312**:883.